Influence of Minimum Count in Brain Perfusion SPECT: Phantom and Clinical Studies

Akie Sugiura[1,2], Masahisa Onoguchi[2], Takayuki Shibutani[2], and Yasuhisa Kouno[1]

[1]*Department of Radiological Technology, Kariya Toyota General Hospital, Kariya, Japan; and* [2]*Department of Quantum Medical Technology, Graduate School of Medical Sciences, Kanazawa University, Kanazawa, Japan*

The count per pixel in brain perfusion SPECT images depends on the administered dose, acquisition time, and patient condition and sometimes become low in daily clinical studies. The aim of this study was to evaluate the effect of different acquisition counts on qualitative images and statistical imaging analysis and to determine the minimum count necessary for accurate examinations. **Methods:** We performed a brain phantom experiment simulating normal accumulation of ^{99m}Tc-ethyl cysteinate dimer as a brain uptake of 5.5%. The SPECT data were acquired in a continuous repetitive rotation. Ten types of SPECT images with different acquisition counts were created by varying the number of rotations added. We used normalized mean squared error and visual analysis. For the clinical study, we used images of 25 patients. The images were acquired in a continuous repetitive rotation, and we created 6 brain images with different acquisition counts by varying the number of rotations added from 1 to 6. The contrast-to-noise ratio was calculated from the mean counts within regions of interest in gray and white matter. In addition, the severity, extent, and ratio of disease-specific regions were evaluated as indices of statistical imaging analysis. **Results:** For the phantom study, the curve of normalized mean squared error tended to converge from approximately 23.6 counts per pixel. Furthermore, the visual score showed that images with 23.6 counts per pixel or less were barely diagnosable. For the clinical study, the contrast-to-noise ratio was significantly decreased at 11.5 counts per pixel or less. Severity and extent tended to increase with decreasing acquisition counts, and a significant increase was shown at 5.9 counts per pixel. On the other hand, there was no significant difference in ratios among different acquisition counts. **Conclusion:** On the basis of a comprehensive assessment of phantom and clinical studies, we suggest that 23.6 counts per pixel or more are necessary to maintain the quality of qualitative images and to accurately calculate indices of statistical imaging analysis.

Key Words: brain perfusion imaging; statistical imaging analysis; artifact; acquisition counts; SPECT

J Nucl Med Technol 2022; 50:342–347
DOI: 10.2967/jnmt.122.264058

Brain perfusion SPECT has an important role in diagnosing the severity of cerebral vascular disorders, determining their prognosis, and identifying dementia, which contribute to clinical management of patients (*1*). SPECT has a lower spatial resolution than morphologic neuroimaging techniques such as CT and MRI but allows for visualization and quantification of brain function and metabolism, which are difficult to evaluate by other modalities.

In addition to visual interpretation, SPECT images can be interpreted using statistical image analysis such as 3-dimensional stereotactic surface projections (*2*) and statistical parametric mapping (*3*). In these widely applied methods, the individual brain image is transformed into a template and the relative regional uptake is compared voxel by voxel with the reference database to generate the *z* score of hypoperfusion (*4*). The results are projected onto the brain surface to create a surface representation of the *z* score (*5*), which facilitates diagnosis in areas that are difficult to assess visually (*6*).

However, counts per pixel in brain perfusion SPECT images depend on the administered dose, acquisition time, and patient condition and sometimes become low in daily clinical studies. It is well known that statistical noise has a significant impact on image quality. The relationship between statistical noise (N) and counts per pixel (n) is expressed as $N = \sqrt{n}/n \times 100$ (*7*), where the signal-to-noise ratio of the SPECT image is proportional to the square root of all counts. As the number of acquisition counts decreases, statistical noise increases and image quality deteriorates.

The purpose of this study was to evaluate the effect of different acquisition counts on qualitative images and statistical imaging analysis and to determine the minimum acquisition count necessary for accurate examinations. When clinical limitations result in low acquisition counts, we can attend to interpretation of the qualitative images and the indices. Although published studies are available on the influence of acquisition and reconstruction methods (*8–10*), this is the first time—to our best knowledge—that minimum acquisition count has been addressed.

MATERIALS AND METHODS

Phantom Design

A Hoffman 3-dimensional brain (Kyoto Kagaku Co., Ltd.) that simulates gray-matter and white-matter structures with a 4:1 activity concentration was used as the phantom (*11*). This phantom was filled with a 37 kBq/mL solution of ^{99m}Tc. The total activity in the phantom was 44.4 MBq at the acquisition start. There is assumed to be a normal accumulation of ^{99m}Tc-ethyl cysteinate dimer with

Received Feb. 23, 2022; revision accepted Jun. 29, 2022.
For correspondence or reprints, contact Masahisa Onoguchi (onoguchi@staff.kanazawa-u.ac.jp).
Published online Jun. 30, 2022.

a dose of 822 MBq as a brain uptake of 5.5% (*12*). The dose was determined with reference to the subjects used in the clinical studies.

Patients

Images of 25 patients (16 men and 9 women; mean age, 75 ± 11.3 y) who underwent resting-state brain perfusion ^{99m}Tc-ethyl cysteinate dimer SPECT from March 2016 to March 2019 were retrospectively used. These patients had degenerative nerve diseases (n = 22) or cerebrovascular diseases (n = 3). The imaging diagnosis indicated decreased cerebral blood flow in all cases. Permission for this study was obtained from the hospital ethics committee.

Image Acquisition

In both phantom and clinical studies, the SPECT acquisition was performed with a dual-head γ-camera (Discovery NM/CT 670 Q.Suite Pro; GE Healthcare Japan) equipped with a low-energy high-resolution collimator. The main energy window was 140.5 keV ± 10% width. The subwindows were set at 159.5 keV ± 3% and 121.5 keV ± 4% for scatter correction. The matrix size was 128 × 128, and the pixel size was 2.94 mm (×1.5 zoom). The data were acquired in continuous mode in a 360° circular orbit (radius of rotation, 150 mm) and 90 projections of a 4° step angle.

For the phantom study, the SPECT acquisition time was set as 3.5 min with 6 rotations and, subsequently, as 7.5 min with 16 rotations (Fig. 1A). For the clinical study, ^{99m}Tc-ethyl cysteinate dimer (Fujifilm Toyama Chemical Co., Ltd.) of 805 ± 40.1 MBq was injected intravenously; 15 min later, images were acquired for 6 rotations at 3.5 min per projection (Fig. 1B).

Image Reconstruction

The SPECT images were reconstructed using filtered backprojection with a Ramachandran filter in the phantom and clinical studies. A Butterworth filter (order, 16; cutoff frequency, 0.55 cycles/cm) was used for the prefilter for smoothing. The cutoff frequency of 0.55 cycles/cm was optimized in advance by calculating the normalized mean squared error (NMSE) from high-quality images with a long acquisition time. Attenuation correction with the Chang method was performed assuming a uniform attenuation coefficient of 0.13 cm^{-1} and a 10% attenuation threshold. The triple-energy-window method (*13*) was used for scatter correction. All images were reconstructed on a workstation using Xeleris, version 3.1 (GE Healthcare Japan).

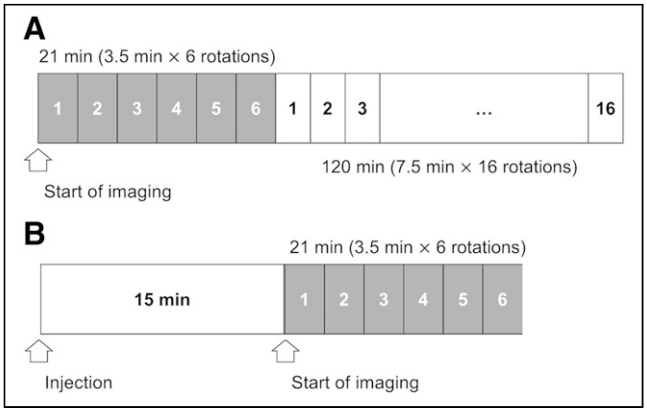

FIGURE 1. SPECT acquisition protocols in this study. (A) Phantom study. Images are acquired for 3.5 min with 6 rotations and subsequently 7.5 min with 16 rotations. (B) Brain perfusion SPECT protocol using ^{99m}Tc-ethyl cysteinate dimer in clinical study. Images are acquired for 21 min [(3.5 min/rotation) × 6 rotations], beginning 15 min after injection.

Image Evaluation

To measure the mean acquisition counts (counts per pixel), we drew a region of interest (ROI) surrounding whole brain on the anterior planar image of the projection data for the phantom (Fig. 2A) (*14*). Brain images were created with 10 different acquisition counts (123.6, 92.3, 61.0, 30.8, 23.6, 19.9, 16.0, 12.0, 7.9, and 4.0 counts per pixel). The NMSE and visual analysis were used to assess each phantom image.

NMSE. The NMSE is given using the following equation:

$$\mathrm{NMSE} = \frac{\sum_{x=0}^{x=n-1}\sum_{y=0}^{y=m-1}(f(x,y)-g(x,y))^2}{\sum_{x=0}^{x=n-1}\sum_{y=0}^{y=m-1}f(x,y)^2},$$

where $f(x,y)$ is equal to the ideal image, $g(x,y)$ is equal to each phantom image, m means matrix size for y, and n means matrix size for x. In this study, the ideal image was created by projections with high acquisition counts (123.6 counts per pixel) to reduce the statistical noise. To precisely assess the convergence of the NMSE in relation to acquisition counts, we evaluated the derivative value of NMSE.

Visual Analysis. Using visual analysis, we scored 10 types of brain images on the basis of how high the counts were. Five observers with expertise in nuclear medicine interpreted the transverse images (Fig. 3) To reduce variability in visual analysis, pretraining was performed using sample images. At that time, we told the observers to assume clinical use, not scientific use, and to observe the cortical accumulation. In a masked manner, they assessed all series and scored them using a scale of 0–4 (4, very good; 3, sufficient for diagnosis; 2, barely diagnosable; 1, cannot be diagnosed responsibly; 0, cannot be diagnosed). The average score for all observers was calculated. The color lookup table was set to inverted grayscale, and the upper and lower limits of the window level were set to 0% and 100%, respectively. Furthermore, enlargement and reduction of the images, observation distance, and observation time were arbitrary. We obtained written consent for all observers to participate in this study.

By varying the number of added rotations on a workstation, we created 6 patient brain images comprising different acquisition counts. The mean acquisition counts were measured by setting an ROI on the normal or mild side on the anterior planar image of the projection data (Fig. 2B) (*14*). Patient images with a minimum of 30 counts per pixel were used. From the results of NMSE and

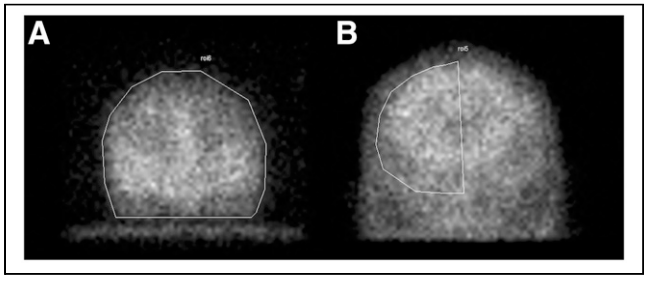

FIGURE 2. (A) ROI for phantom study set to surround whole brain on anterior planar image of projection data. (B) ROI for clinical study set to surround normal or mild side on anterior planar image of projection data.

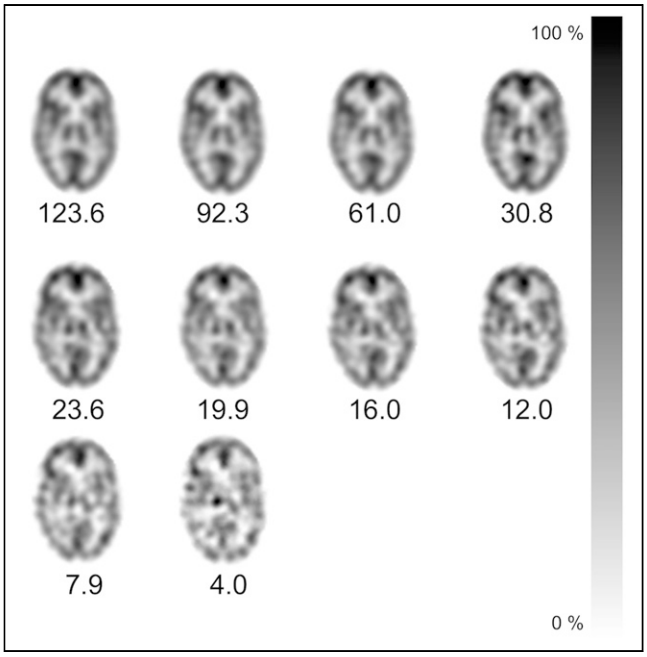

FIGURE 3. Representative slices of images for visual analysis. Images were created from 10 types of projection data with different acquisition counts (123.6, 92.3, 61.0, 30.8, 23.6, 19.9, 16.0, 12.0, 7.9, and 4.0 counts per pixel).

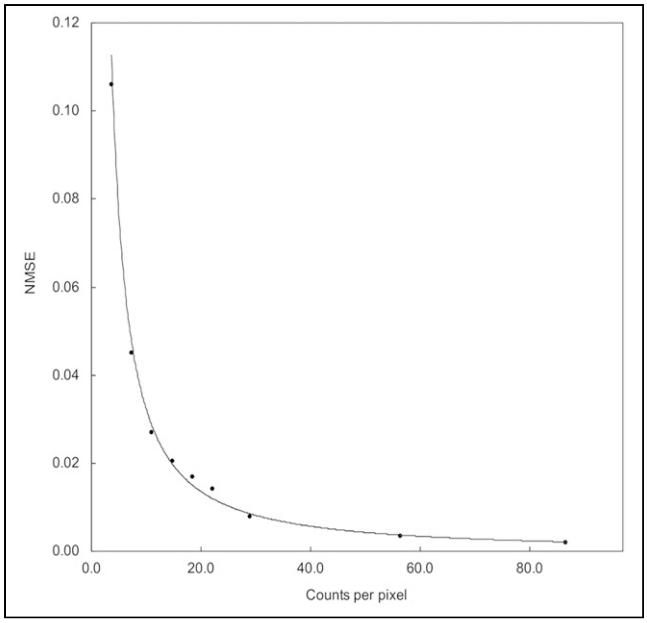

FIGURE 4. NMSE as function of counts per pixel in brain phantom.

visual analysis, we determined the image with 30 counts per pixel or more to be sufficient for diagnosis.

We used the contrast-to-noise ratio (CNR) and the indices from the easy *z* score imaging system (eZIS) (*4*) to assess the influence of low acquisition counts on qualitative images and statistical imaging analysis.

CNR. ROIs were automatically drawn on transverse images using the 3-dimensional stereotactic ROI template software, and average reconstructed image counts were calculated by dividing the brain into 12 segments (*15*). The CNR is given using the following equation:

$$\mathrm{CNR} = (\text{decreases in rCBF signal} - \text{background}) / \text{standard division (background)},$$

where decreases in regional cerebral blood flow (rCBF) signal are the average reconstructed-image counts in an ROI surrounding the areas diagnosed as decreases in rCBF on brain perfusion SPECT, background is the average reconstructed image counts of cerebellum ROIs, and standard division (background) is the standard division of cerebellum ROIs (*16*). Therefore, patients with decreases in rCBF in the cerebellum were excluded from the study. The CNR was obtained from the 6 brain images and normalized by the value of the 6-rotation image.

eZIS Analysis. eZIS analysis discriminates early Alzheimer disease from other types of dementia using computer-assisted statistical analysis. The indices of eZIS that characterize decreases in rCBF in patients with very early Alzheimer disease—namely severity, extent, and ratio—were calculated, automatically analyzing the specific volume of interest (VOI) in the posterior cingulate gyrus, precuneus, and parietal cortices. The severity and extent show the degree and percentage of rCBF decrease in the VOI. The ratio shows the percentage of rCBF decrease in the VOI to a whole brain. The severity, extent, and ratio were obtained from 6 brain images of different acquisition counts for each patient and were normalized by the values of the 6-rotation image. Patients with degenerative nerve diseases ($n = 22$) were analyzed because eZIS was used in the differential diagnosis of dementia. We performed the eZIS analysis using a Daemon research image processor, version 1.1.0.0 (DRIP; Fujifilm Toyama Chemical Co., Ltd.)

Statistical Analysis

All statistical analyses were performed using the statistical package EZR (version 1.38) (*17*). Visual scores were compared for differences using the Kruskal–Wallis/Steel test. Wilcoxon signed-rank testing with the Bonferroni adjustment was used to analyze CNR, severity, extent, and ratio among all image sets. A *P* value of less than 0.01 was considered statistically significant.

RESULTS

Phantom Study

In the curve of NMSE in relation to acquisition counts, a tendency toward convergence was observed with increasing acquisition counts (Fig. 4). The curve of the derivative value of NMSE rapidly increased at low acquisition counts, followed by saturation as close to zero as possible above 23.6 counts per pixel (Fig. 5).

The visual score increased with increasing acquisition counts and showed a score higher enough than "2, barely diagnosable" at 23.6 counts per pixel or more and a score higher enough than "3, sufficient for diagnosis" at 30 counts per pixel or more (Fig. 6).

Clinical Study

The CNR was significantly decreased at 11.5 counts per pixel or less ($P < 0.01$, Table 1).

Severity and extent tended to increase with decreasing acquisition counts, and a significant increase was shown at

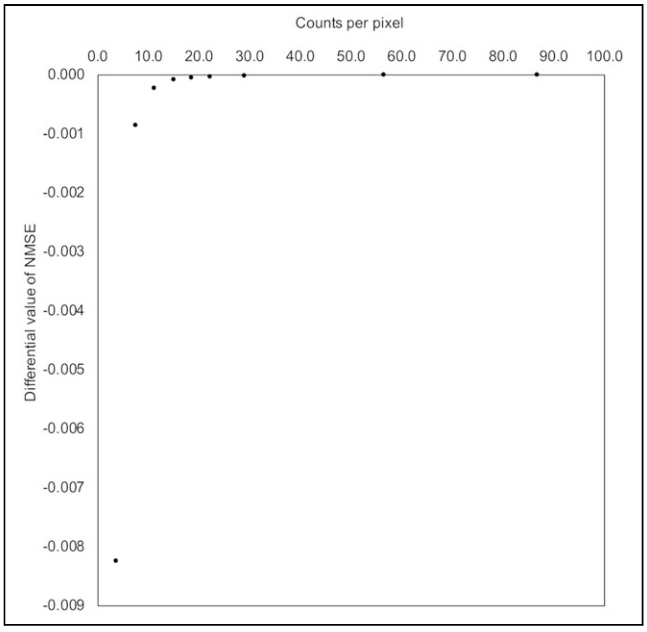

FIGURE 5. Differential value of NMSE as function of counts per pixel.

5.9 counts per pixel ($P < 0.01$). On the other hand, ratio was independent of acquisition counts, and there was no significant difference in ratios among acquisition counts (Table 2). Differences in the average counts per pixel between Tables 1 and 2 were caused by differences in the numbers of patients analyzed in CNR and eZIS analysis. Figure 7 compares the 6-rotation image (32.9 counts per pixel) with the image obtained at a low acquisition count (6.2 counts per pixel) using statistical imaging analysis.

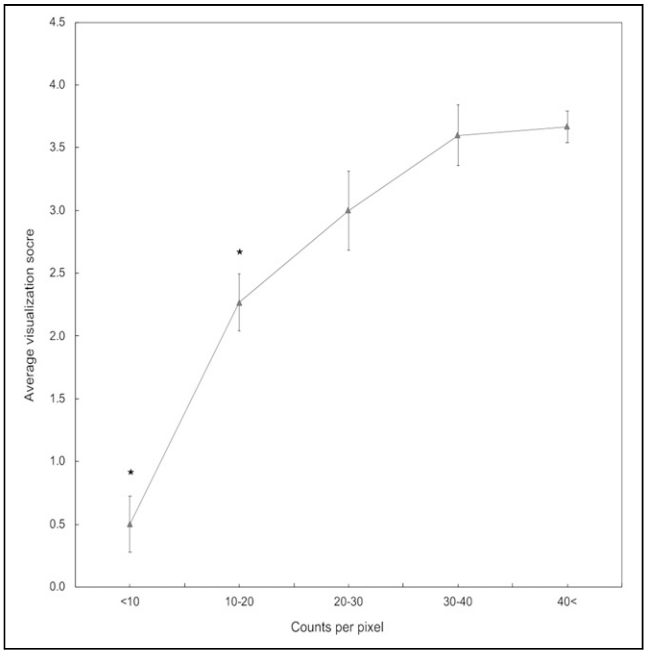

FIGURE 6. Relationship between average visualization score and each range of counts per pixel. *Versus 40 counts per pixel or more, $P < 0.01$.

DISCUSSION

Recent dementia practice guidelines recommend use of morphologic imaging (MRI or CT) to exclude neurosurgical dementia and then use of functional imaging (brain perfusion SPECT or dopamine transporter scintigraphy) to make a differential diagnosis (*18*). Brain perfusion SPECT is commonly used in differential diagnosis of dementia to assess the pattern of hypoperfusion for each type of dementia and is also expected to be used for early diagnosis of Alzheimer disease in patients with mild cognitive impairment (*19*). On the other hand, in daily practice for patients with dementia, the characteristic symptoms may force interruption or shortening of the scan. A consequence is that they sometimes lead to low acquisition counts. Therefore, it is important to study the effects of different acquisition counts and to determine the minimum count necessary for accurate examinations. We believe that our study will prove useful in daily clinical practice.

Much previous research has dealt with improving image quality in brain perfusion SPECT by reducing image noise. As a result, it is now possible to obtain images with less statistical noise by optimizing the low-pass filter or using multipinhole collimators (*8,9*). Furthermore, it has been reported that iterative reconstruction technology with resolution recovery algorithms can improve spatial resolution while suppressing statistical noise (*10*). However, studies on decreases in acquisition counts are insufficient, although such decreases may occur in daily clinical practice.

As a result of the phantom study, we considered 23.6 counts per pixel or more necessary to maintain image quality, because the NMSE showed a convergence at 23.6 counts per pixel or more and the score with visual analysis was higher enough than "2, barely diagnosable" at 23.6 counts per pixel or more. NMSE is commonly used to optimize the low-pass filter or the iteration number and well reflects the influence of statistical noise on SPECT images (*8,10*). Furthermore, it was assumed that statistical noise did not affect the ideal image of the NMSE because we reconstructed the ideal image from projection data with statistical noise lower than 10%, applying an optimized Butterworth filter. In addition, visual assessment by scoring is also widely used in nuclear medicine imaging (*20*). Therefore, the obtained results are reliable.

In the clinical study, the value of CNR showed a significant decrease at 11.5 counts per pixel, and we decided that 17.2 counts per pixel or more did not affect the detection of decreases in rCBF. The severity and extent tended to increase with decreasing acquisition counts, and a significant increase was shown at 5.9 counts per pixel ($P < 0.01$). It was assumed that statistical noise was determined as a hypoperfusion area in the specific VOI during eZIS analysis (*21*), and we need to note false-positives in differential diagnosis of dementia using eZIS analysis. We decided that

TABLE 1
Average and SD of CNR at Different Counts per Pixel in patients with degenerative nerve diseases ($n = 22$) and cerebrovascular diseases ($n = 3$)

Parameter	6 rotations	5 rotations	4 rotations	3 rotations	2 rotations	1 rotation
Counts per pixel	33.6 (±4.25)	28.3 (±3.55)	22.7 (±2.86)	17.2 (±2.17)	11.5 (±1.45)	5.9 (±0.73)
Normalized CNR	1.00 (±0.0)	0.99 (±0.08)	0.96 (±0.10)	0.92 (±0.16)	0.84 (±0.17)*	0.56 (±0.25)*

*Versus 33.6 counts per pixel, $P < 0.01$.

TABLE 2
Average and SD of Indices (Severity, Extent, and Ratio) at Different Counts per Pixel in Patients with Degenerative Nerve Diseases ($n = 22$)

Parameter	6 rotations	5 rotations	4 rotations	3 rotations	2 rotations	1 rotation
Counts per pixel	33.9 (±4.45)	28.5 (±3.72)	22.9 (±2.99)	17.3 (±2.28)	11.6 (±1.52)	5.9 (±0.77)
Normalized severity	1.00 (±0.0)	1.01 (±0.05)	1.05 (±0.06)	1.05 (±0.08)	1.07 (±0.15)	1.50 (±0.47)*
Normalized extent	1.00 (±0.0)	1.00 (±0.12)	1.11 (±0.15)	1.18 (±0.55)	1.11 (±0.41)	2.34 (±2.12)*
Normalized ratio	1.00 (±0.0)	0.97 (±0.11)	1.02 (±0.14)	1.01 (±0.51)	0.84 (±0.28)	1.33 (±1.17)

*Versus 33.9 counts per pixel, $P < 0.01$.

11.6 counts per pixel or more did not affect the severity and extent. The minimum acquisition count for severity and extent is lower than that for CNR because of the smoothing process included in the eZIS analysis process (*22*). On the other hand, the ratio was independent of the acquisition counts, suggesting that the statistical noise influenced not only the specific VOI but also the whole brain. The phantom study simulated normal human brain, whereas the clinical study addressed detection of cerebral hypoperfusion.

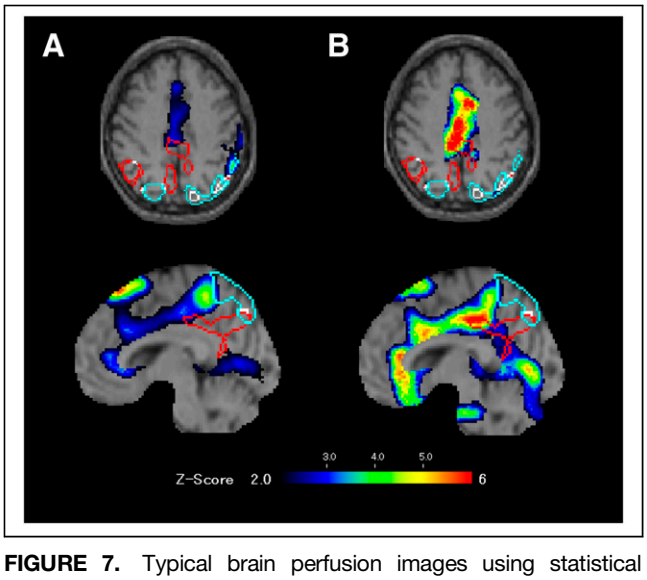

FIGURE 7. Typical brain perfusion images using statistical image analysis obtained at different counts in patient: reference images obtained at 32.9 counts per pixel (A) and images obtained at 6.2 counts per pixel (B). False-positives were observed in specific VOI (red border).

Therefore, we considered that differences occurred between visual analysis in the phantom study and the results of the clinical investigation.

On the basis of comprehensive assessment of phantom and clinical studies, we determined that 23.6 counts per pixel were the minimum to maintain the quality of qualitative images and to accurately calculate indices of statistical imaging analysis. Generally, more than 100 counts per pixel were needed to suppress statistical noise (*7*). Stelter et al. (*23*) also suggested 50 counts per pixel or more for sufficient image quality. We considered that our result differed from previous studies because this research dealt with the minimum acquisition count, not with sufficient image quality. The presence of cerebral ventricles in the ROI that we set may also affect the acquisition counts. For routine brain perfusion SPECT examinations, we recommend using the proposed minimum acquisition count either as the criterion for reexamination or as a warning to the physician.

There were some limitations to this study. First, we categorized 10 types of brain images to 5 scales of image quality by visual analysis, but having 5 scales of image quality is actually vague and may include various aspects of image quality such as observer preference. Therefore, when setting the cutoff for the counts, we selected 30.0 counts per pixel or 23.6 counts per pixel, at which the score was higher enough than 3 or 2 to have margins. Further study should be conducted to clarify the differences in the 5 scales and to reveal the relationship between less-than-ideal image quality and diagnostic accuracy. A second limitation was the difference between the devices. Differences in reconstruction methods, low-pass filters, or various correction methods are surmised to affect the minimum acquisition count.

But we considered the results of statistical imaging analysis to be widely applicable to other devices because the analysis reduces differences between devices by anatomic standardization and smoothing. The minimum acquisition count can lead to precise diagnosis and shorter scan times. Furthermore, in young patients, use of a minimum count is expected to reduce radiation exposure by optimizing the radiopharmaceutical dose. Therefore, in the future, it is desirable to determine the minimum acquisition count, considering differences between devices.

CONCLUSION

On the basis of this comprehensive assessment of phantom and clinical studies, we suggest that 23.6 counts per pixel or more are necessary to maintain the quality of qualitative images and to accurately calculate indices of statistical imaging analysis. The proposed minimum acquisition count will help raise the reliability of brain perfusion SPECT, such as by serving as the criterion for reexamination or as a warning to the physician.

DISCLOSURE

No potential conflict of interest relevant to this article was reported.

ACKNOWLEDGMENT

We thank the staff at the Department of Radiological Technology, Kariya Toyota General Hospital, for technical support.

KEY POINTS

QUESTION: What is the minimum acquisition count for brain perfusion SPECT?

PERTINENT FINDINGS: In this phantom and clinical study, the minimum acquisition count was 23.6 per pixel.

IMPLICATIONS FOR PATIENT CARE: The proposed minimum acquisition count will help raise the reliability of brain perfusion SPECT.

REFERENCES

1. Camargo EE. Brain SPECT in neurology and psychiatry. *J Nucl Med.* 2001;42:611–623.
2. Minoshima S, Frey KA, Koeppe RA, Foster NL, Kuhl DE. A diagnostic approach in Alzheimer's disease using three-dimensional stereotactic surface projections of fluorine-18-FDG PET. *J Nucl Med.* 1995;36:1238–1248.
3. Friston KJ, Frith CD, Fletcher P, Liddle PF, Frackowiak RS. Functional topography: multidimensional scaling and functional connectivity in the brain. *Cereb Cortex.* 1996;6:156–164.
4. Kanetaka H, Matsuda H, Asada T, et al. Effects of partial volume correction on discrimination between very early Alzheimer's dementia and controls using brain perfusion SPECT. *Eur J Nucl Med Mol Imaging.* 2004;31:975–980.
5. Matsuda H, Mizumura S, Nagao T, et al. Automated discrimination between very early Alzheimer disease and controls using an easy *Z* score imaging system for multicenter brain perfusion single-photon emission tomography. *AJNR.* 2007;28:731–736.
6. Imabayashi E, Matsuda H, Asada T, et al. Superiority of 3-dimensional stereotactic surface projection analysis over visual inspection in discrimination of patients with very early Alzheimer's disease from controls using brain perfusion SPECT. *J Nucl Med.* 2004;45:1450–1457.
7. Todd-Pokropek AE, Jarritt PH. The noise characteristics of SPECT systems. In: Ell PJ, Holman BL, eds. *Computed Emission Tomography.* Oxford University Press; 1983:361–389.
8. Minoshima S, Maruno H, Yui N, et al. Optimization of Butterworth filter for brain SPECT imaging. *Ann Nucl Med.* 1993;7:71–77.
9. Chen L, Tsui BM, Mok GS. Design and evaluation of two multi-pinhole collimators for brain SPECT. *Ann Nucl Med.* 2017;31:636–648.
10. Yokoi T, Shinohara H, Onishi H. Performance evaluation of OSEM reconstruction algorithm incorporating three-dimensional distance-dependent resolution compensation for brain SPECT: a simulation study. *Ann Nucl Med.* 2002;16:11–18.
11. Hoffman EJ, Cutler PD, Diby WM, Mazziotta JC. Three dimensional phantom to simulate cerebral blood flow and metabolic images for PET. *IEEE Trans Nucl Sci.* 1990;37:616–620.
12. Kubo A, Nakamura K, Tsukatani Y, et al. Phase I clinical study of ^{99m}Tc-ECD. *Kaku Igaku.* 1992;29:1019–1027.
13. Ogawa K, Harata Y, Ichihara T, Kubo A, Hashimoto S. A practical method for position-dependent Compton-scattered correction in single photon emission CT. *IEEE Trans Med Imaging.* 1991;10:408–412.
14. Yamanaga T, Hasegawa S, Imoto A, et al. Guidelines for standardization of brain perfusion SPECT imaging 1.0. *Kakuigaku Gijutsu.* 2017;37:505–516.
15. Takeuchi R, Yonekura Y, Matsuda H, Konshi J. Usefulness of a three-dimensional stereotaxic ROI template on anatomically standardised ^{99m}Tc-ECD SPET. *Eur J Nucl Med Mol Imaging.* 2002;29:331–341.
16. Matsuda H, Mizumura S, Nagao T, et al. An easy Z-score imaging system for discrimination between very early Alzheimer's disease and controls using brain perfusion SPECT in a multicentre study. *Nucl Med Commun.* 2007;28:199–205.
17. Kanda Y. Investigation of the freely available easy-to-use software 'EZR' for medical statistics. *Bone Marrow Transplant.* 2013;48:452–458.
18. Ngo J, Holroyd-Leduc JM. Systematic review of recent dementia practice guidelines. *Age Ageing.* 2015;44:25–33.
19. Ito K, Mori E, Fukuyama H, et al. Prediction of outcomes in MCI with ^{123}I-IMP-CBF SPECT: a multicenter prospective cohort study. *Ann Nucl Med.* 2013;27:898–906.
20. Fukukita H, Suzuki K, Matsumoto K, et al. Japanese guideline for the oncology FDG-PET/CT data acquisition protocol: synopsis of version 2.0. *Ann Nucl Med.* 2014;28:693–705.
21. Yanamoto T, Onishi H, Murakami T, Takahashi M, Odajima S, Uchida K. Research report: accuracy and evaluation of the stereotactic statistical imaging analysis of the brain. *Nippon Hoshasen Gijutsu Gakkai Zasshi.* 2008;64:752–765.
22. Yamamoto Y, Onoguchi M. Statistical image analysis method to use for cerebral blood flow SPECT examination: difference and matters that require attention of processing of eZIS and iSSP. *Nippon Hoshasen Gijutsu Gakkai Zasshi.* 2011;67:718–727.
23. Stelter P, Junik R, Krzyminiewski R, Gembicki M, Sowin'ski J. Semiquantitative analysis of SPECT images using ^{99}Tc^{m}-HMPAO in the treatment of brain perfusion after the attenuation correction by the Chang method and the application of the Butterworth filter. *Nucl Med Commun.* 2001;22:857–865.